Brazilian Dental Science

unesp
UNIVERSIDADE ESTADUAL PAULISTA
"JÚLIO DE MESQUITA FILHO"
Instituto de Ciência e Tecnologia
Campus de São José dos Campos

Original Article DOI: https://doi.org/10.4322/bds.2026.e4995

Analysis of fracture resistance and surface characteristics of bioactive ceramic cluster filler and bulk fill fiber-reinforced composites in endodontically treated teeth

Análise da resistência à fratura e caracterização de superfície de compósitos a base de carga cerâmica bioativa do tipo cluster e bulk- fill reforçados por fibras em dentes tratados endodonticamente

Maulida HAYATI[1,2], Nurhayaty NATSIR[1], Aries Chandra TRILAKSANA[1]

1 - Hasanuddin University, Faculty of Dentistry, Department of Dental Conservation. Makassar, South Sulawesi, Indonesia.
2 - Baiturrahmah University, Faculty of Dentistry. Padang, West Sumatera, Indonesia.

How to cite: Hayati M, Natsir N, Trilaksana AC. Analysis of fracture resistance and surface characteristics of bioactive ceramic cluster filler and bulk fill fiber-reinforced composites in endodontically treated teeth. Braz. Dent. Sci. 2026;29:e4995. https://doi.org/10.4322/bds.2026.e4995

ABSTRACT

Objective: This study aimed to compare the mechanical, surface, and interfacial properties of a bioactive ceramic cluster filler composite (TMR-Z Fill 10) and a fiber-reinforced bulk-fill composite (EverX Posterior) in ETT, with intact teeth serving as controls. **Material and Methods:** Forty-five extracted maxillary premolars were divided into three groups (n = 15): intact teeth, TMR-Z Fill 10 restorations, and EverX Posterior restorations. Fracture resistance was measured using a universal testing machine. Surface roughness and morphology were analyzed by atomic force microscopy (AFM). Interface gaps and elemental composition were evaluated using scanning electron microscopy and energy-dispersive spectroscopy (SEM-EDS). Mineralization profiles were determined with Fourier-transform infrared spectroscopy (FTIR). Data were analyzed using one-way ANOVA and Post-Hoc Tukey HSD ($p < 0.05$). **Results:** Fracture resistance of TMR-Z Fill 10 (1760.86 ± 330.31 N) was comparable to intact teeth (1785.84 ± 367.25 N) and significantly higher than EverX Posterior (1491.96 ± 275.91 N; $p < 0.05$). AFM revealed smoother surfaces on composites than on enamel, with TMR-Z Fill 10 showing greater uniformity. SEM demonstrated narrower gaps in EverX (3.60 ± 0.43 μm) than in TMR-Z Fill 10 (8.40 ± 0.82 μm). EDS confirmed bioactive ion release from both composites, while FTIR indicated fluoride-mediated remineralization in TMR-Z Fill 10 but weaker carbonate stability in EverX. **Conclusion:** TMR-Z Fill 10 preserved fracture resistance and supported remineralization, whereas EverX Posterior provided superior marginal adaptation. Neither material fully replicated intact teeth, but each exhibited distinct advantages for restoring ETT.

KEYWORDS

Bioactive composite; Endodontically treated teeth; Fiber-reinforced composite; Fracture resistance; Interface gap.

RESUMO

Objetivo: Este estudo teve como objetivo comparar as propriedades mecânicas, de superfície e interfaciais de um compósito com carga cerâmica bioativa tipo cluster (TMR-Z Fill 10) e de um compósito bulk-fill reforçado com fibras (EverX Posterior) em DTE, utilizando dentes íntegros como controle. **Material e Métodos:** Quarenta e cinco pré-molares superiores extraídos foram divididos em três grupos (n = 15): dentes íntegros; restaurações com TMR-Z Fill 10; e restaurações com EverX Posterior. A resistência à fratura foi avaliada em uma máquina de ensaio universal. Rugosidade e morfologia de superfície foram analisadas por microscopia de força atômica (MFA). Lacunas na interface e composição quimica foram avaliadas por microscopia eletrônica de varredura e espectroscopia de dispersão de energia (MEV-EDS). Perfis de mineralização foram determinados por espectroscopia infravermelho transformada de Fourier (FTIR). Os dados foram analisados por ANOVA one-way e Post-Hoc Tukey HSD ($p < 0,05$). **Resultados:** A resistência à fratura do TMR-Z Fill 10 (1760,86 ± 330,31 N) foi comparável à dos dentes íntegros (1785,84 ± 367,25 N) e significativamente maior que a do EverX Posterior (1491,96 ± 275,91 N; $p < 0,05$). A MFA revelou superfícies mais lisas nos compósitos em relação ao esmalte, com maior uniformidade no TMR-Z Fill 10. O MEV mostrou lacunas menores no EverX (3,60 ± 0,43 μm) do que no TMR-Z Fill 10 (8,40 ± 0,82 μm). O EDS confirmou a liberação de íons bioativos por ambos os compósitos, enquanto a FTIR indicou remineralização mediada por flúor no TMR-Z Fill 10, mas menor estabilidade de carbonato no EverX. **Conclusão:** O TMR-Z Fill 10 preservou a resistência à fratura e favoreceu a remineralização, enquanto o EverX Posterior apresentou melhor adaptação marginal. Nenhum dos materiais replicou completamente os dentes íntegros, mas cada um apresentou vantagens específicas para a restauração de DTE.

PALAVRAS-CHAVE

Compósito bioativo; Dentes tratados endodonticamente; Compósito reforçado com fibras; Resistência à fratura; Lacuna na interface.

INTRODUCTION

Restoration of endodontically treated teeth (ETT) remains one of the most demanding challenges in restorative dentistry. Loss of tooth structure following endodontic access preparation, instrumentation, and obturation procedures inevitably alters biomechanical behavior, reduces fracture resistance, and compromises the long-term prognosis of the tooth [1]. Without adequate reinforcement, ETTs are more susceptible to catastrophic fractures, marginal leakage, and restorative failure under functional loading [2]. These concerns highlight the need for restorative materials that not only restore form and function but also provide mechanical reinforcement and biological integration [3].

Over the past decade, several composite technologies have been introduced to address these issues. Fiber-reinforced composites (FRCs), such as EverX Posterior, incorporate short glass fibers into a resin matrix to improve crack deflection, distribute occlusal stresses, and increase fracture toughness [4]. Laboratory investigations have demonstrated that FRCs enhance load-bearing capacity; however, their heterogeneous fiber matrix configuration may compromise surface uniformity and interfacial sealing, thereby influencing plaque retention and marginal adaptation [5]. In parallel, bioactive ceramic cluster filler composites, such as TMR-Z Fill 10, have emerged with the ability to release calcium, phosphate, and fluoride ions. These ions not only buffer acidic challenges but also promote remineralization of the adjacent tooth structure, potentially reducing micro-gap formation and improving adhesive integration [6]. Despite these advancements, the comparative performance of these novel composites in ETT is not yet fully established.

Previous research has primarily focused on fracture resistance alone, whereas fewer studies have combined mechanical, surface, and chemical analyses within a single experimental framework [7]. In particular, limited evidence is available comparing the balance between structural reinforcement and interfacial adaptation provided by bioactive ceramic cluster fillers and fiber-reinforced bulk-fill composites. This gap in the literature restricts clinicians from making evidence-based decisions regarding the most suitable restorative material for compromised teeth [8].

The novelty of the present study lies in its comprehensive, multi-level evaluation of restorative performance. By integrating fracture resistance testing with atomic force microscopy (AFM) surface analysis, scanning electron microscopy combined with energy-dispersive X-ray spectroscopy (SEM-EDS) for interfacial characterization, and Fourier-transform infrared spectroscopy (FTIR) for mineralization profiling, this study provides holistic insights into both the mechanical and bioactive behavior of these materials. Such an approach allows direct comparison with intact teeth, serving as a natural benchmark for restorative success. Accordingly, the general objective of this study was to evaluate and compare the mechanical properties, surface characteristics, and interfacial adaptation of a bioactive ceramic cluster filler composite (TMR-Z Fill 10) and a fiber-reinforced bulk-fill composite (EverX Posterior) in endodontically treated teeth. The null hypothesis tested was that there would be no significant differences in fracture resistance, surface roughness, interface gap, or mineralization potential among the tested composites and intact teeth.

MATERIALS AND METHODS

Research design

An in vitro experimental design with a post-test only control group was used. A total of 45 extracted human maxillary premolars indicated for orthodontic treatment were collected, cleaned, and stored in 0.9% saline solution. The teeth were randomly divided into three groups (n = 15 each): intact tooth (Control), restoration with TMR-Z Fill 10, and restoration with EverX Posterior.

Sample preparation

Forty-five extracted maxillary premolars were cleaned with a hand scaler and stored in 0.9% saline at 4°C. Each tooth was embedded in self-cure acrylic resin (Vertex Dental, Zeist, Netherlands) with the cemento-enamel junction positioned 2 mm above the resin surface. Endodontic access cavities were prepared using a high-speed handpiece. Root canals were instrumented with ProTaper Next rotary files (Dentsply-Maillefer, Ballaigues, Switzerland) to size X2 (#25) with irrigation using 2.5% NaOCl (Paragon, Jakarta, Indonesia), 17% EDTA (Meta Biomed, Cheongju, South Korea), and distilled water.

The canals were dried, obturated with ProTaper Next X2 gutta-percha and AH-Plus sealer (Dentsply DeTrey, Konstanz, Germany) using the single-cone technique, and sealed coronally with resin-modified glass ionomer cement. Standardized mesio-occluso-distal (MOD) cavities (6 mm depth, bucco-palatal width one-third intercuspal distance, gingival floor 1 mm) were prepared with diamond burs under water cooling. A circumferential matrix system (Palodent 360, Dentsply Sirona, Ballaigues, Switzerland) was applied before restoration [9].

Restorative procedures

For the TMR-Z Fill 10 group, cavities were rinsed with distilled water, gently air-dried, and conditioned with TMR-AQUA BOND 0 self-etch adhesive (Yamakin, Osaka, Japan), which was air-thinned and light-cured for 10 s. TMR-Z Fill 10 Universal composite (Yamakin, Japan) was placed in 2-mm increments and light-cured for 10 s per layer using a SmartLite® Pro Modular LED curing light (Dentsply Sirona; 1,250 mW/cm^2). For the EverX Posterior group, G-Premio Bond adhesive (GC Corp., Tokyo, Japan) was applied, air-thinned for 5 s, and light-cured for 5 s. The proximal box was restored with G-ænial Posterior composite (GC Corp., Tokyo, Japan) and light-cured for 10 s. EverX Posterior was then placed in up to 4-mm increments, followed by an occlusal capping layer of G-ænial Posterior; each increment was light-cured for 10 s [10]. Increment thickness followed manufacturer-recommended clinical protocols: TMR-Z Fill 10 was applied in 2-mm layers to ensure adequate polymerization and minimize shrinkage stress, whereas EverX Posterior, a bulk-fill short fiber-reinforced composite used as a dentin substitute, was applied in up to 4-mm increments and capped with a conventional posterior composite to optimize occlusal anatomy and surface finish.

Finishing and polishing protocol

All restored specimens underwent standardized finishing and polishing performed by a single calibrated operator. Finishing was carried out using fine-grit diamond burs under continuous water cooling. Polishing was then performed using a multi-step polishing system with sequential discs from coarse to superfine grit (e.g., Sof-Lex™, 3M ESPE), each applied for 20–30 s under constant pressure. Final polishing was completed using a polishing paste and felt disc for 30 s. After polishing, specimens were rinsed and ultrasonically cleaned in distilled water for 5 minutes, then air-dried before AFM and SEM evaluation.

Fracture resistance assay

The specimens were embedded in resin blocks with the cemento-enamel junction positioned 2 mm above the resin surface. Fracture resistance was evaluated using a universal testing machine (Shimadzu GS-X, 5 kN, Japan) by applying a vertical compressive load with a 5-mm-diameter steel ball at a crosshead speed of 1 mm/min until fracture occurred, and the maximum fracture load was recorded in Newtons (N) [11]. All restorations were performed by a single calibrated operator following a standardized protocol. The light-curing unit output (1,250 mW/cm^2) was verified before the procedures, and curing was performed with the light tip positioned perpendicular to the restoration surface at a standardized distance (approximately 0–1 mm) for the specified exposure time. All specimens were restored using the same matrix system and cavity geometry, with identical adhesive protocols applied within each material group to minimize procedural variability.

AFM assay

Surface roughness of the restorations was analyzed using an Atomic Force Microscope (NX10, Park Systems Corp., Suwon, South Korea) operated in tapping mode. Three representative specimens per group were randomly selected, gently rinsed, and ultrasonically cleaned in distilled water for 5 minutes to remove surface debris, then air-dried. The specimens were mounted on AFM stubs using double-sided adhesive to minimize vibration. Surface topography was recorded over a $10 \times 10\,\mu$m scanning area, and roughness parameters (Ra, Rq, Rp, Rv, Ry) were obtained at three standardized sites per specimen. The mean value per specimen was calculated, and data were expressed as mean ± standard deviation for statistical analysis [12].

SEM-EDX assay

EDS results were expressed as both atomic percentage (At%) and weight percentage (Wt%) to provide complementary information on elemental distribution and mass contribution of inorganic fillers. Longitudinal sections of each specimen were examined under a scanning electron microscope (JSM-6510LV, JEOL Ltd., Tokyo, Japan) at 5000× magnification. The interface gap between tooth structure and restoration was measured using ImageJ software (NIH, Bethesda, MD, USA).

Five measurements were obtained from each specimen, averaged, and expressed as mean ± standard deviation. The occurrence of micro-cracks and voids along the adhesive interface was also documented. Elemental composition at the interface was analyzed using energy-dispersive X-ray spectroscopy (X-MaxN 20, Oxford Instruments, Abingdon, UK) attached to the SEM. Both atomic percent (At%) and weight percent (Wt%) values were determined. The elements assessed included calcium (Ca), phosphorus (P), oxygen (O), zirconium (Zr), silicon (Si), and fluoride (F), while the Ca/P ratio was calculated to evaluate mineral content and interfacial adaptation [13].

FTIR assay

Powdered samples obtained from the restoration-tooth interface were analyzed with Fourier-transform infrared spectroscopy (IRTracer-100, Shimadzu Corp., Kyoto, Japan). Spectra were recorded over 4000–400 cm^{-1} with a resolution of 4 cm^{-1} and 32 scans per specimen. Peaks associated with phosphate (PO_4^{3-}), carbonate (CO_3^{2-}), and fluoride (~878 cm^{-1}) were identified and compared among groups [14].

Statistical analysis

Data were analyzed using SPSS version 26.0 (IBM Corp., Armonk, NY, USA). Data normality was assessed using the Shapiro–Wilk test. One-way analysis of variance (ANOVA) was used to compare group means. For parameters showing a statistically significant overall ANOVA ($p < 0.05$), post hoc multiple comparisons were conducted using the Tukey honestly significant difference (HSD) test to control for type I error. No post-hoc analysis was performed when the ANOVA result was not statistically significant. Statistical significance was set at $p < 0.05$.

Ethical clearance

The study protocol was reviewed and approved by the Ethics Committee of the Faculty of Dentistry, Universitas Hasanuddin, Indonesia, under approval number 122/KEPK FKG-RSGM UH/EE/V/2025. All procedures involving extracted human teeth were performed in accordance with the ethical principles of the Declaration of Helsinki. Written informed consent for the use of teeth was obtained from patients before extraction.

RESULTS

Table I shows the mean fracture resistance (±SD) of the three experimental groups. The Control group (intact teeth) demonstrated the highest fracture resistance (1785.84 ± 367.25 N), followed closely by the TMR-Z Fill 10 group (1760.86 ± 330.31 N), while the EverX Posterior group showed the lowest values (1491.96 ± 275.91 N). Statistical analysis using one-way ANOVA revealed significant differences among the groups ($p = 0.032$). Post-hoc LSD indicated no significant difference between the Control and TMR-Z Fill 10 groups (ns), but both groups exhibited significantly higher fracture resistance compared to EverX Posterior ($p < 0.05$).

Fracture pattern analysis (Figure 1) showed that intact teeth and the TMR-Z Fill 10 group predominantly exhibited restorable fractures, defined as fractures confined to the coronal portion of the tooth or restoration above the cemento-enamel junction (CEJ), allowing the possibility of clinical re-restoration. In contrast, the EverX Posterior group was dominated by non-restorable fractures, defined as fractures extending below the CEJ and/or involving the root structure, which would clinically indicate extraction.

Table II shows that intact teeth had the highest surface roughness (Ra = 0.300 μm), reflecting natural enamel prisms, while both composites were smoother: EverX Posterior (0.069 μm) and TMR-Z Fill 10 (0.088 μm). Although ANOVA showed no significant difference ($p > 0.05$), EverX exhibited higher variability due to fiber exposure, whereas TMR-Z Fill demonstrated greater uniformity from ceramic cluster fillers.

Table I - Fracture resistance of composite resin restoration

Group	N	Mean ± SD (N)	* p-value	Post-Hoc (LSD)	Remarks
Control (Intact Teeth)	15	1785.84 ± 367.25		vs TMR: 0.835 (ns) vs EverX: 0.018*	Similar to TMR, significantly higher than EverX
TMR-Z Fill 10 (Ceramic)	15	1760.86 ± 330.31	0.032*	vs Control: 0.835 (ns) vs EverX: 0.029*	Comparable to intact teeth, superior to EverX
EverX Posterior	15	1491.96 ± 275.91		vs Control: 0.018* vs TMR: 0.029*	Significantly lower fracture resistance

*One-Way ANOVA. ANOVA revealed significant differences among groups ($p < 0.05$).

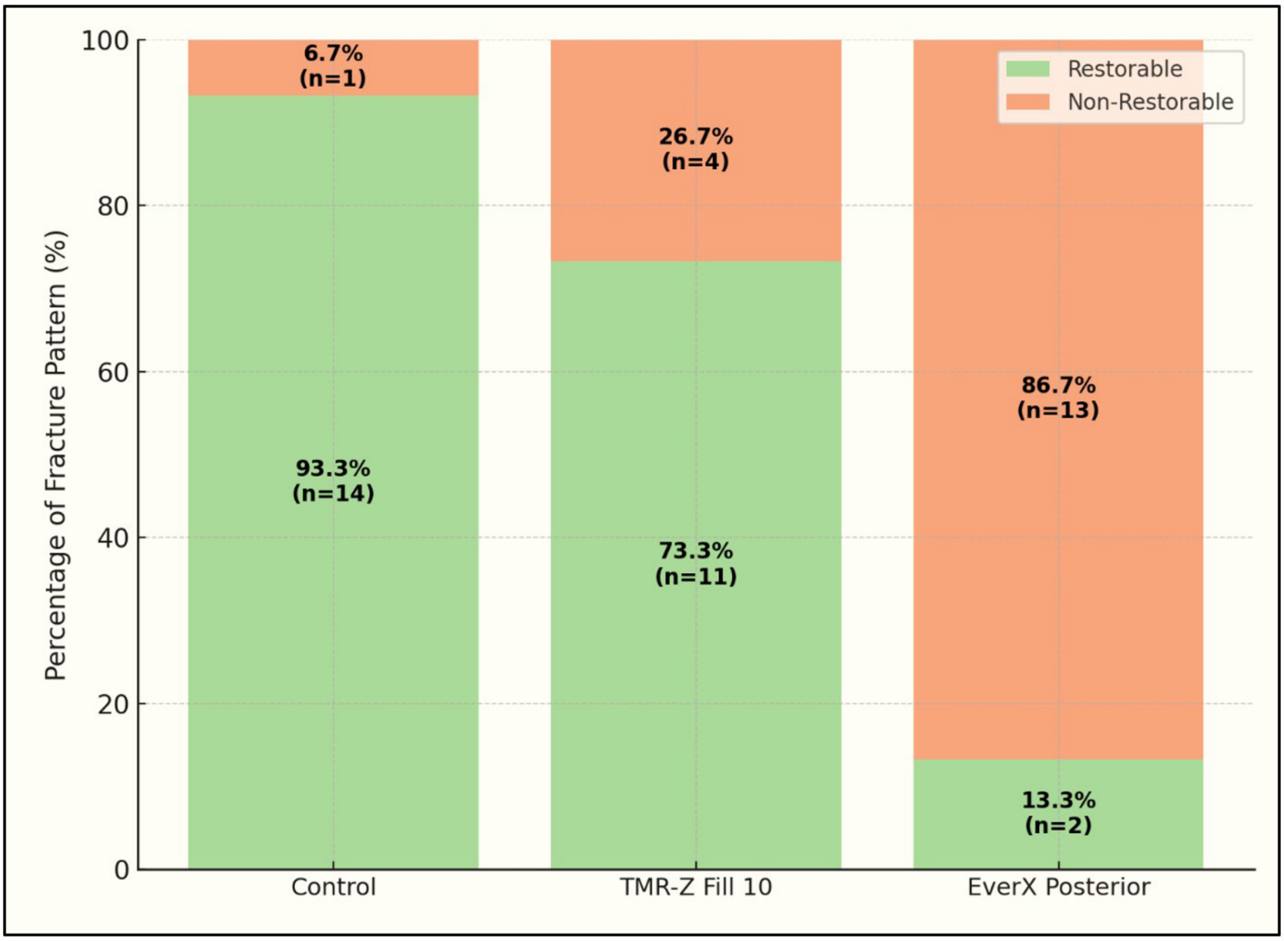

Figure 1 - Distribution of fracture patterns among experimental groups. Fracture patterns were classified as restorable fractures, defined as fractures confined to the coronal portion of the tooth or restoration above the cemento-enamel junction (CEJ), and non-restorable fractures, defined as fractures extending below the CEJ and/or involving the root structure, which would clinically indicate extraction. Intact teeth (Control) showed predominantly restorable fractures (93.3%, n = 14), followed by the TMR-Z Fill 10 group (73.3%, n = 11). In contrast, the EverX Posterior group exhibited a high proportion of non-restorable fractures (86.7%, n = 13). Percentages and absolute counts (n) are shown within each bar.

Table II - Surface Roughness Parameters of composite resin restoration

Group	n	Surface Roughness (μm)					*p-value
		Mean Ra± SD	Rq	Rp	Rv	Ry	
Control (Intact Teeth)	3	0.300 ± 0.000	0.3800	1.600	0.850	0.770	
TMR-Z Fill 10 (Ceramic)	3	0.088 ± 0.012	0.1095	0.365	0.240	0.270	0.084
EverX Posterior	3	0.069 ± 0.041	0.0815	0.304	0.224	0.155	

*One-way ANOVA revealed no statistically significant difference in surface roughness (Ra) among the Control, TMR-Z Fill 10, and EverX Posterior groups ($p > 0.05$).

Figure 2 shows AFM images of surface morphology. EverX Posterior displayed irregular topography with exposed fibers, whereas TMR-Z Fill 10 had a smoother, more uniform surface due to evenly distributed ceramic clusters. The control enamel appeared roughest due to its natural prism structure. These findings confirm the roughness data, indicating that TMR-Z Fill 10 offers better polishability and esthetic potential, whereas EverX may require additional finishing to reduce surface irregularities.

Table III shows that EverX Posterior had the smallest interface gaps (3.60 ± 0.43 μm) with good marginal sealing, while TMR-Z Fill 10 showed the widest gaps (8.40 ± 0.82 μm), indicating poorer adaptation despite uniform filler distribution. The control group showed no adhesive gap, only minor natural micro-cracks. ANOVA confirmed significant group differences ($p < 0.001$), highlighting EverX's better sealing ability compared to TMR-Z.

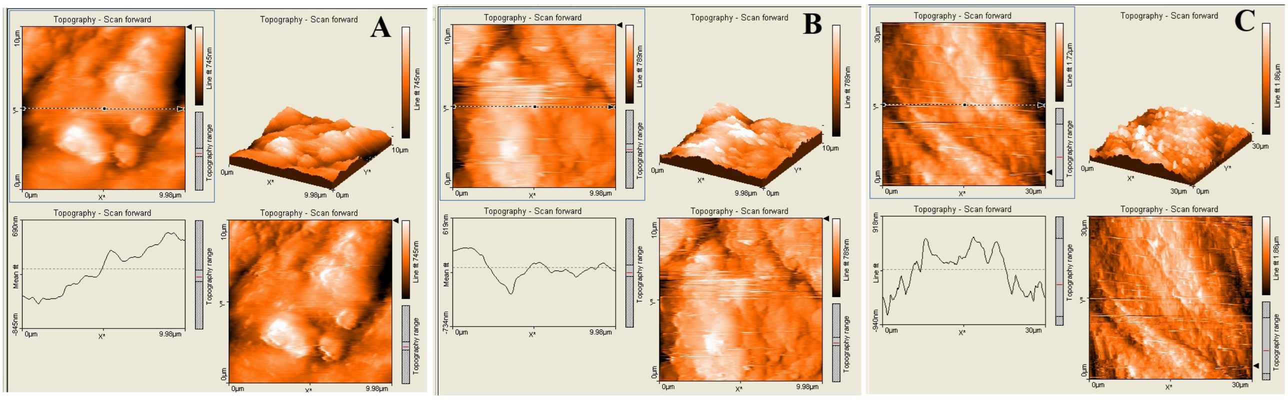

Figure 2 - AFM analysis of composite resin restorations and control enamel. (A) EverX Posterior; (B) TMR-Z Fill 10, and (C) Control (intact teeth). All images were obtained from sample 1 in each group and are presented as representative surface topographies for roughness evaluation.

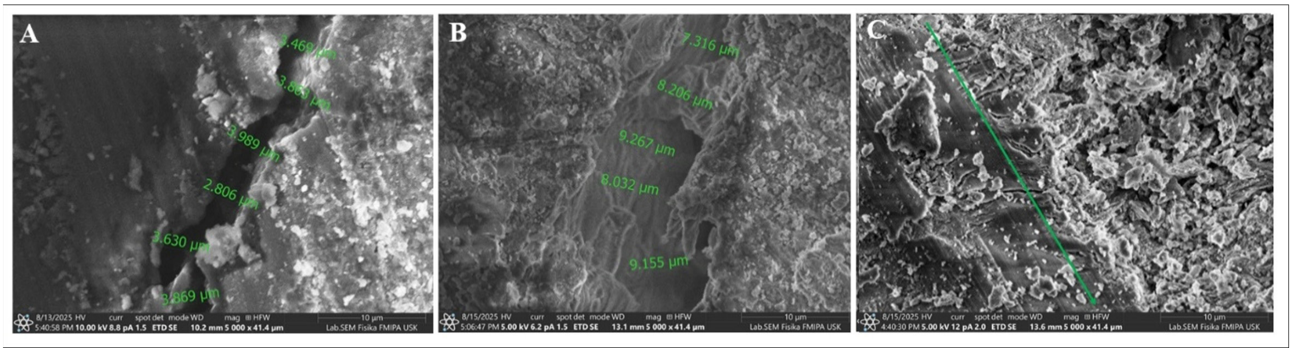

Figure 3 - SEM micrographs of interface gap analysis at 5000× magnification. (A) EverX Posterior showed narrow gaps (2.8–3.9 µm); (B) TMR-Z Fill 10 displayed wider gaps (7.3–9.3 µm); and (C) control teeth had no gaps, only natural enamel microcracks.

Table III - SEM Interface Gap Analysis of composite resin restoration

Group	N	Mean ± SD (µm)	Range (µm)	Interface Gap Adhesive	Micro-cracks / Voids	*p-value
Control (Intact Tooth)	3	0.00 ± 0.00	0.00 – 0.00	Not found	Small sporadic micro-cracks (<1–1.5 µm)	
TMR-Z Fill 10 (Ceramic)	3	8.40 ± 0.82	7.32 – 9.27	Present (wider, irregular)	Minimal, homogeneous filler zones	0.001
EverX Posterior	3	3.60 ± 0.43	2.81 – 3.99	Present (narrow, continuous)	Minor, linked to fiber exposure	

*One-Way ANOVA

Figure 3 shows that EverX Posterior had narrow, continuous adhesive gaps (2.8–3.9 μm), indicating better marginal sealing. TMR-Z Fill 10 displayed wider gaps (7.3–9.2 μm), reflecting poorer adaptation despite uniform fillers. The control group showed no adhesive gap, only natural micro-cracks. Overall, EverX achieved superior sealing compared to TMR-Z, though neither matched the sealing of intact teeth.

Table IV shows that the control group was dominated by Ca, P, and O, consistent with hydroxyapatite. EverX Posterior contained higher levels of silica and fluoride, supporting its fiber-reinforced, remineralizing, and antibacterial properties. TMR-Z Fill 10 featured zirconium and silica, confirming ceramic cluster fillers with retained Ca–P bioactivity. Additional Zn and S peaks suggest antimicrobial and strengthening effects.

Figure 4 shows clear elemental differences: the control group was dominated by Ca, P, O, and C, reflecting natural hydroxyapatite; TMR-Z Fill 10 contained zirconium and silica, confirming its ceramic cluster filler design; and EverX Posterior showed silica with detectable fluoride, indicating its fiber-reinforced, fluoride-releasing composition. These spectra confirm the distinct bioactive and structural roles of each material.

Table V shows that the control teeth had strong phosphate and carbonate peaks, confirming well-mineralized hydroxyapatite.

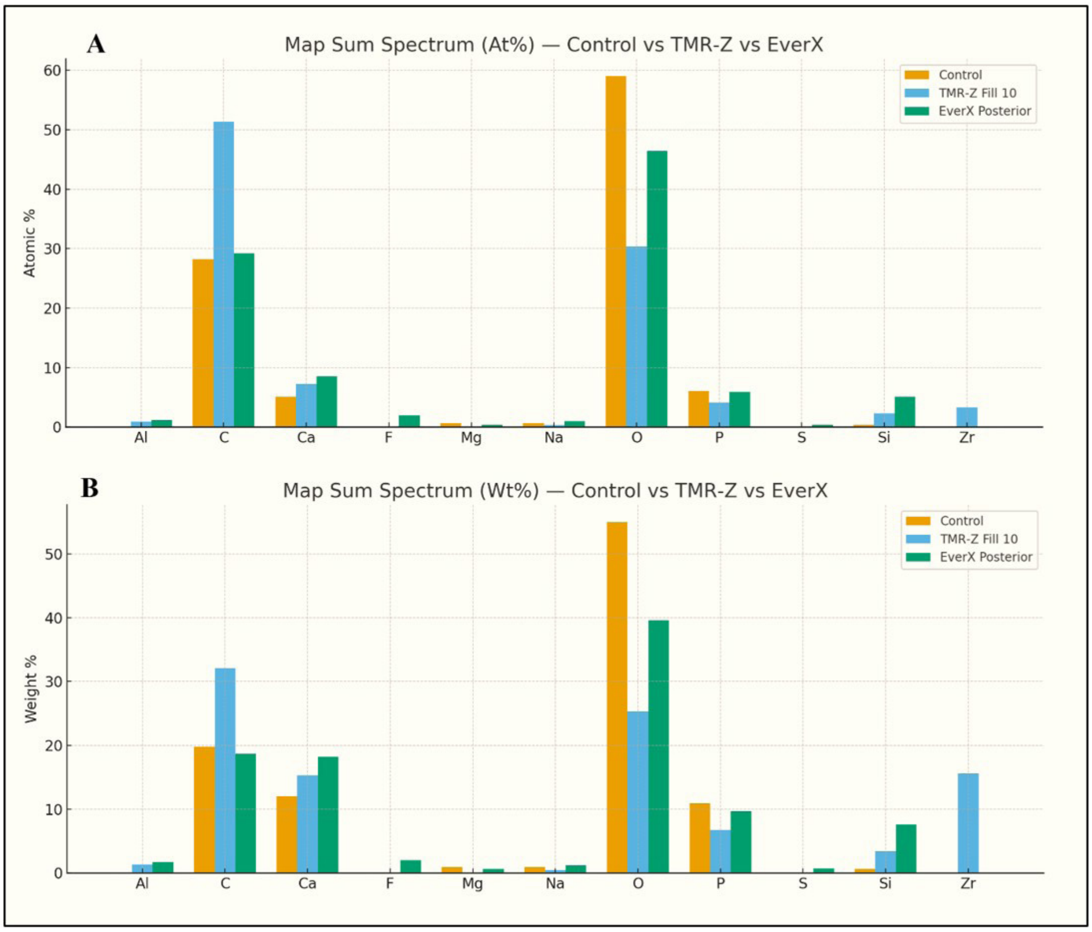

Figure 4 - Comparative EDS Map Sum Spectrum of Control (intact tooth), (A) Atomic percentage shows Control dominated by Ca–P–O, TMR-Z enriched with Zr and Si, and EverX with Si and F; (B) Weight percentage confirms these profiles: hydroxyapatite in Control, zirconium in TMR-Z, and silica-fluoride in EverX.

Table IV - EDS Map Sum Spectrum of composite resin restoration

Group / Material	Major Elements (At% / Wt%)	Characteristic Elements	Interpretation
Control (Intact Tooth)	O (59.0 / 55.0), C (28.2 / 19.8), P (6.0 / 10.9), Ca (5.1 / 12.0)	Ca, P, O (Hydroxyapatite)	Mineral dominated by Ca–P consistent with hydroxyapatite. Minor Mg, Na, Si as natural enamel trace elements.
TMR-Z Fill 10 (Ceramic)	O (30.4 / 25.3), C (51.3 / 32.1), Ca (7.3 / 15.3), P (4.1 / 6.7), Zr (3.3 / 15.6), Si (2.3 / 3.4)	Zr, Si, Al	The presence of zirconium (Zr) and silica (Si) indicates ceramic-based filler clusters. Balanced Ca–P contributes to bioactivity.
EverX Posterior	O (46.4 / 39.6), C (29.2 / 18.7), Ca (8.5 / 18.2), Si (5.1 / 7.6), P (5.9 / 9.7), F (1.9 / 2.0)	Si, F, Zn	Fiber-reinforced matrix enriched with silica and fluoride release, suggesting potential remineralization and antibacterial effect.
Other Composite Regions (Bioactive zones)	O (33.7), C (59.2), Ca (4.1), Si (3.1), P (2.9), Zn (0.8), S (0.5)	Zn, S	Indicates bioactive filler modification with Zn and S, possibly for antimicrobial and strengthening purposes.

Data Source: Own research 2025.

Table V - FTIR Analysis of Tooth Mineralization on the Interface Gap Area

Group	Main FTIR Peaks (cm^{-1})	Interpretation
Control (Intact Tooth)	1040–1090 (PO_4^{3-} stretching), 960 (PO_4^{3-} symmetric), 1420–1460 (CO_3^{2-} stretching)	Strong hydroxyapatite and carbonate bands indicate optimal natural mineralization.
TMR-Z Fill 10 (Ceramic)	1040–1090 (PO_4^{3-}), 1420–1460 (CO_3^{2-}), additional shoulder ~875–880 (F^- interaction with phosphate)	The presence of fluoride-associated peaks suggests bioactive remineralization and reduced micro-gap at the interface.
EverX Posterior	1040–1090 (PO_4^{3-}), reduced 1420–1460 (CO_3^{2-}) intensity, weak/absent F^- peak	Lower carbonate and weaker phosphate bonding imply less stable remineralization, consistent with a wider micro-gap interface.

Data Source: Own research 2025.

TMR-Z Fill 10 displayed similar peaks with an additional fluoride-related shoulder (~878 cm^{-1}), indicating enhanced remineralization and better interfacial adaptation. EverX Posterior, however, showed weaker carbonate peaks and no fluoride signal, suggesting less stable mineralization. TMR-Z Fill 10 demonstrated superior bioactive remineralization, while EverX relied more on mechanical reinforcement with limited bioactivity.

Figure 5 illustrates the FTIR comparison among the intact tooth, TMR-Z Fill 10, and EverX Posterior. The control spectrum demonstrated strong phosphate and carbonate absorption bands, confirming optimal mineralization associated with hydroxyapatite in enamel and dentin. In TMR-Z Fill 10, similar phosphate and carbonate peaks were observed, but the additional shoulder around 878 cm^{-1} signified the presence of fluoride ions released from ceramic cluster fillers. This fluoride-associated feature suggests enhanced remineralization and bioactivity at the tooth–restoration interface. In contrast, the EverX Posterior spectrum showed weaker carbonate bands and no detectable fluoride peak, suggesting less stable remineralization despite the presence of phosphate peaks.

Table VI presents the post-hoc Tukey HSD analysis for fracture resistance and interface gap parameters. Fracture resistance did not differ significantly between the Control and TMR-Z Fill 10 groups, whereas both groups exhibited significantly higher fracture resistance than EverX Posterior ($p < 0.05$). For interface gap measurements, both restorative groups showed significantly larger gaps than the Control, with TMR-Z Fill 10 exhibiting significantly wider interface gaps than EverX Posterior ($p < 0.05$).

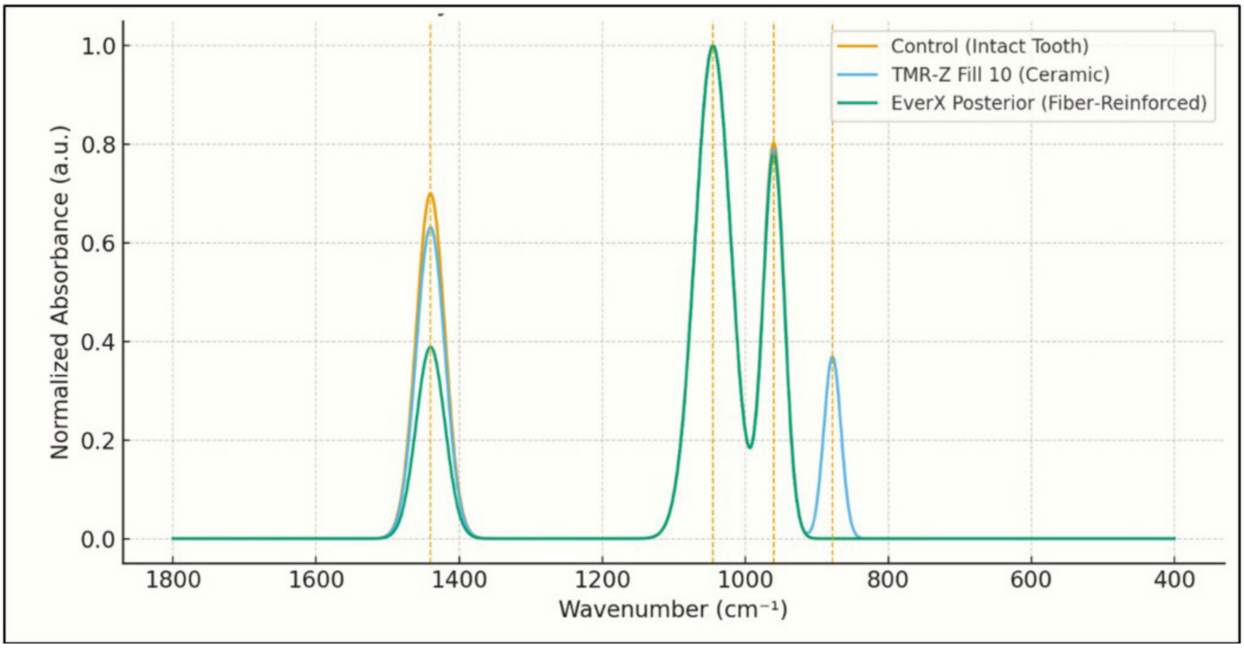

Figure 5 - FTIR spectra (overlay) of Control (intact tooth), TMR-Z Fill 10, and EverX Posterior within the wavenumber range 1800–400 cm^{-1}. Control showed strong phosphate and carbonate peaks, indicating intact hydroxyapatite. TMR-Z Fill 10 showed similar peaks, along with a fluoride shoulder (~878 cm^{-1}), suggesting enhanced remineralization. EverX showed weaker carbonate and no fluoride peak, reflecting less stable mineralization.

Table VI - Post-Hoc Tukey HSD Results for Fracture Resistance and Interface Gap

Parameter	Comparison	Mean Difference	p-value	Remarks
Fracture Resistance (N)	Control vs TMR-Z Fill 10	24.98	0.835 (ns)	No significant difference
	Control vs EverX Posterior	293.88	0.018*	Control > EverX
	TMR-Z Fill 10 vs EverX Posterior	268.90	0.029*	TMR-Z > EverX
Interface Gap (μm)	Control vs EverX Posterior	3.60	0.0017*	EverX > Control
	Control vs TMR-Z Fill 10	8.40	0.0046*	TMR-Z > Control
	EverX Posterior vs TMR-Z Fill 10	4.80	0.0109*	TMR-Z > EverX

*Significant at $p < 0.05$; ns = not significant. Post-hoc pairwise comparisons were conducted using the Tukey HSD test only for parameters with a significant overall ANOVA result.

DISCUSSION

The present study demonstrated that TMR-Z Fill 10 exhibited fracture resistance comparable to that of intact teeth, whereas EverX Posterior showed significantly lower values. This finding suggests that ceramic-cluster fillers are more effective at restoring biomechanical strength in endodontically treated teeth (ETT) than short-fiber reinforcement. Similar outcomes were reported by researchers, who emphasized that filler architecture and chemistry strongly influence crack initiation and load distribution [15]. Ceramic-based fillers with high filler loading improve stiffness and enhance crack deflection, allowing the material to mimic natural tooth behavior under occlusal forces. In contrast, the performance of short-fiber reinforced composites (sFRCs) largely depends on fiber orientation, length, and interfacial bonding with the resin matrix, which explains the relatively lower resistance observed in the EverX group [16].

Recent systematic reviews also support this interpretation, noting that although sFRCs can increase fracture resistance in weakened teeth, the outcomes remain inconsistent and technique-sensitive [17]. Other studies highlighted that cavity design, remaining wall thickness, and restorative technique play critical roles in determining whether fibers contribute effectively to reinforcement [18]. Optimizing fiber placement and thickness improved sFRC performance, and bulk application without proper capping or layering could compromise its load-bearing capacity [19]. Taken together, these results suggest that ceramic-cluster composites such as TMR-Z Fill 10 offer a more robust and technique-tolerant reinforcement for MOD-prepared ETT [20]. In contrast, sFRCs may achieve comparable outcomes only when strict placement protocols are followed [21].

The fracture pattern analysis in this study was limited to a clinically oriented classification (restorable vs non-restorable). Although more detailed fracture classifications (e.g., adhesive, cohesive, mixed, or bone-level based systems) and statistical analysis of fracture distribution could provide additional mechanistic insight, the present approach was selected to emphasize clinical decision-making relevance. The descriptive nature of fracture pattern assessment and the limited sample size represent limitations of this study and should be addressed in future investigations.

Fracture pattern analysis revealed that intact teeth predominantly exhibited restorable fractures (93.3%), reflecting the natural resilience of enamel–dentin structures. In comparison, TMR-Z Fill 10 maintained a relatively high proportion of restorable fractures (73.3%), suggesting that its ceramic cluster fillers effectively reinforced tooth structure and favored repairable failure modes. In contrast, EverX Posterior demonstrated mostly non-restorable fractures (86.7%), indicating a tendency toward catastrophic failure despite fiber reinforcement. These findings align with previous studies showing that ceramic-based bioactive composites promote more favorable fracture modes through improved stress distribution and interfacial stability [22]. In contrast, the performance of short-fiber reinforced composites depends heavily on fiber orientation and bonding quality, which may explain their less predictable outcomes [23].

In this study, enamel (Control) exhibited the highest roughness (Ra 0.300 μm). In contrast, both composites were smoother, with EverX Posterior (0.069 μm) and TMR-Z Fill 10 (0.088 μm) below the commonly cited plaque-retention threshold of $\sim$0.2 μm; AFM images corroborated these quantitative trends (Figure 1). Lower Ra is clinically desirable because it reduces biofilm adhesion and improves color stability and gloss. Recent trials and reviews have reiterated that composite surfaces maintained at or below a 0.2 μm limit prevent early bacterial retention and staining [24]. AFM has been emphasized as an appropriate modality for capturing micro- to nanoscale topographies and validating finishing/polishing outcomes [25].

Material-driven explanations align with our observations: TMR-Z Fill 10's more uniform topography (lower SD) is consistent with reports that minor, evenly distributed ceramic/cluster fillers yield smoother, more homogeneous surfaces after finishing and polishing [26]. By contrast, short-fiber-reinforced systems can display localized peaks/valleys where fibers approach or breach the surface, increasing heterogeneity when finishing parameters or layering are suboptimal, an effect noted across the contemporary F/P literature and composite roughness studies [16]. Collectively, these data suggest that while both materials achieve clinically acceptable smoothness, TMR-Z Fill 10 offers more consistent polishability. In contrast, EverX Posterior may require stricter finishing protocols to minimize fiber-related surface irregularities [27].

Although no statistically significant difference in surface roughness was detected among groups, qualitative AFM observations suggested differences in surface uniformity: TMR-Z Fill 10 showed a more homogeneous topography, while EverX Posterior exhibited localized irregularities associated with fiber exposure. These observations are descriptive in nature and should not be interpreted as statistically significant.

In our SEM assessment, no adhesive gap was observed in intact teeth, whereas EverX Posterior exhibited narrow, continuous gaps (3.60 ± 0.43 μm), and TMR-Z Fill 10 showed significantly wider gaps (8.40 ± 0.82 μm). This pattern is consistent with reports that short-fiber–reinforced composites can improve interfacial adaptation by redistributing polymerization stresses and deflecting microcracks along the adhesive interface, provided that fiber volume and placement are appropriate [28]. At the same time, marginal gap formation is multifactorial; matrix systems, cavity geometry, and bulk-fill strategies influence adaptation, with several recent studies showing that particular matrix techniques and bulk placement can either reduce or exacerbate gap widths in Class II restorations [29]. Our measured EverX values align with this literature, indicating favorable sealing when the fiber-reinforced material is layered and appropriately capped.

Conversely, the larger gaps in TMR-Z Fill 10 may reflect higher effective polymerization shrinkage stress or less compatible adhesive interaction despite its bioactive design. Contemporary reviews emphasize that resin-composite shrinkage and stress development are governed by filler architecture, resin chemistry, and conversion kinetics; depending on cluster morphology and modulus, ceramics-rich systems can accumulate interfacial stress if compliance or bonding is suboptimal [30]. Although TMR-Z Fill 10 incorporates ceramic cluster fillers with sustained fluoride release features intended to promote remineralization at the tooth–restoration interface, such chemical benefits do not necessarily translate into smaller immediate gaps if shrinkage stress is not adequately managed during curing [31]. Our findings, therefore, fit a broader trend: fiber-reinforced composites can yield better marginal adaptation than ceramics-cluster systems under specific techniques, even when the latter may excel in other properties (e.g., fracture resistance), and internal adaptation itself is sensitive to placement protocol and curing strategy [32].

EDS mapping in this study showed the control group dominated by Ca, P, and O—an elemental triad characteristic of hydroxyapatite in enamel–dentin, while EverX Posterior was enriched with Si (silica phase) and detectable F, and TMR-Z Fill 10 presented Zr- and Si-bearing ceramic clusters with a balanced Ca–P signal. These signatures are consistent with current understanding of dental hard tissues and restorative fillers: enamel's mineral phase is predominantly hydroxyapatite (Ca–P–O), as reiterated by recent overviews of enamel composition and structure [33], whereas composite performance is tightly linked to filler chemistry and morphology [34].

The functional implications align with contemporary literature on bioactive and fiber-reinforced systems. EverX's Si- and F-containing profile supports fluoride availability and a siliceous reinforcement phase that can contribute to antibacterial effects and remineralization potential, echoing reports on fluoride-releasing or F-doped composite technologies [35]. Conversely, the Zr- and Si-rich clusters detected in TMR-Z Fill 10 reflect the manufacturer-reported ceramic cluster strategy intended to combine mechanical reinforcement with sustained ion release [20], in line with broader reviews linking filler composition to both mechanical and biological Performance [36]. Together, these findings explain the complementary behaviors observed elsewhere in this study: EverX favored marginal adaptation, whereas TMR-Z preserved load-bearing capacity while exhibiting a bioactive chemical profile [37]. Although fluoride was more prominently detected in EverX Posterior by EDS, the potential remineralization behavior of TMR-Z Fill 10 was interpreted based on its Ca–P balance and ceramic cluster filler composition rather than fluoride content alone.

The FTIR band observed around 875–880 cm^{-1} is more appropriately assigned to the ν_2 carbonate mode of apatite, which may indicate mineral-phase reorganization rather than direct evidence of fluoride-mediated remineralization [38]. FTIR profiling corroborated compositional differences among groups. The control spectrum showed well-defined phosphate bands (ν3 PO4 at ~1040–1090 cm^{-1}; ν1 PO4 at ~960 cm^{-1}) and a carbonate band near ~1440 cm^{-1}, consistent with the hydroxyapatite signature of enamel–dentin reported by Orilisi et al. and others. In TMR-Z Fill 10, phosphate and carbonate features were also evident, with an additional shoulder in the ~875–880 cm^{-1} region.

Although the ~878 cm^{-1} band is classically assigned to the v2 carbonate mode in apatites and bioactive glass–derived precipitates (rather than a discrete "fluoride peak"), its emergence/intensification has been linked to ion-exchange–driven surface reprecipitation and lattice reorganization during remineralization, processes facilitated in fluoride-releasing systems [39]. Taken together with our EDS data and prior reports on bioactive composites, these spectra support the interpretation that TMR-Z promotes mineral deposition at the interface.

By contrast, EverX Posterior showed weaker carbonate intensity and no discernible shoulder near 878 cm^{-1} in our conditions, suggesting less stable interfacial mineral formation despite the presence of phosphate bands. Contemporary studies emphasize that fluoride-releasing restorative materials enhance remineralization adjacent to restorations and can improve marginal integrity under demineralizing challenges [40]. Our FTIR trends align with this literature: TMR-Z's ion-releasing/ceramic-cluster design favored chemical integration, whereas EverX relied predominantly on mechanical reinforcement with limited bioactive spectral signatures.

Mechanically, our finding that a ceramic-cluster composite can approximate intact teeth while an sFRC lags is compatible with recent syntheses showing that filler architecture and resin–filler coupling drive load transfer and crack control [41]. Meta-analyses on ETT also note that fiber reinforcement benefits depend on technique, fiber volume, orientation, and capping protocols, explaining why sFRCs do not uniformly outperform other systems [1]. On the surface level, both composites achieved Ra values below the plaque-retention threshold (~0.2 μm), supporting favorable biofilm behavior [42]. The greater uniformity seen for TMR-Z aligns with reports that evenly distributed ceramic/cluster fillers polish more consistently than fiber-containing matrices, which may exhibit localized peaks where fibers approach the surface [43].

Interfacially, EverX's narrower continuous gaps are consistent with the literature, which shows that short fibers can redistribute shrinkage stresses and improve marginal adaptation when used with appropriate placement and capping strategies [44]. Conversely, larger gaps with TMR-Z are compatible with models linking polymerization shrinkage stress to resin chemistry and cluster morphology when compliance or bonding is suboptimal [45]. Chemically, EDS/FTIR indicated complementary strengths: TMR-Z evidenced a bioactive profile (Zr/Si clusters with ion release and an FTIR shoulder in the 875–880 cm^{-1} region suggesting interfacial mineral reprecipitation), while EverX showed Si with detectable F. Still, weaker carbonate features findings that mirror contemporary reviews on bioactive RBCs and fluoride-mediated remineralization at restoration margins [46]. Clinically, material selection for ETT should reflect the primary objective: prioritize TMR-Z when maximal load-bearing and bioactivity are paramount, and consider EverX when marginal adaptation is the primary concern, both paired with strict protocol control to optimize outcomes.

These findings underscore a clinically relevant trade-off between potential bioactivity and marginal adaptation. Although bioactive restorative materials are designed to interact chemically with the surrounding tooth structure, this bioactive potential does not necessarily translate into superior initial interfacial sealing. In the present study, TMR-Z Fill 10 demonstrated features consistent with ion-mediated interactions that may support remineralization; however, these observations were derived from single-time-point analyses. Therefore, the findings should be interpreted with caution, and longitudinal investigations are required to verify whether such interactions result in sustained remineralization and long-term improvement of marginal integrity under clinical conditions. A limitation of this study is the use of a single post hoc approach in the initial analysis and the absence of inferential statistics for the distribution of fracture patterns. Future studies should consider applying more conservative post hoc tests and conducting formal statistical analyses of fracture modes using standardized classification systems

CONCLUSION

TMR-Z Fill 10 restored fracture resistance close to intact teeth, promoted bioactive remineralization, and favored restorable fractures. At the same time, EverX Posterior showed weaker strength but better marginal sealing, though mostly non-restorable fractures. Neither fully replicated natural enamel, but TMR-Z offered mechanical and bioactive benefits, whereas EverX provided superior interface adaptation, making material choice dependent on clinical priorities.

Acknowledgements

The authors would like to express their sincere gratitude to the Faculty of Dentistry, Universitas Hasanuddin, for providing laboratory facilities, as well as to the Biomedical Laboratory of Universitas Syiah Kuala (USK) for technical support in AFM, SEM-EDS, and FTIR analyses. Appreciation is also extended to all staff and colleagues who contributed to the preparation and completion of this research.

Data availability

The data that support the findings of this study are available from the corresponding author upon reasonable request.

Author's Contributions

MH: Conceptualization, Methodology, Investigation, Data Curation, Formal Analysis, Visualization, Writing – Original Draft Preparation. NN: Supervision, Validation, Writing – Review & Editing, Project Administration. ACT: Resources, Software, Funding Acquisition, Validation, Writing – Review & Editing.

Conflict of Interest

No conflicts of interest declared concerning the publication of this article.

Funding

This research received no external financial support.

Regulatory Statement

Ethical approval was required for this study.

REFERENCES

1. Caussin E, Izart M, Ceinos R, Attal JP, Beres F, François P. Advanced material strategy for restoring damaged endodontically treated teeth: a comprehensive review. Materials (Basel). 2024;17(15): 3736. https://doi.org/10.3390/ma17153736. PMid:39124400.
2. Mishra L, Francis T, Nooji D, Aggarwal H, McColl E, Eachempati P. Current concepts in restoring endodontically treated teeth. Dent Update. 2025;52(1):26-34. https://doi.org/10.12968/denu.2025.52.1.26.
3. Jefferies SR. Bioactive and biomimetic restorative materials: a comprehensive review. Part I. J Esthet Restor Dent. 2014;26(1):14-26. https://doi.org/10.1111/jerd.12069. PMid:24341542.
4. Alshabib A, Jurado CA, Tsujimoto A. Short fiber-reinforced resin-based composites (SFRCs); Current status and future perspectives. Dent Mater J. 2022;41(5):647-54. https://doi.org/10.4012/dmj.2022-080. PMid:35858793.
5. Rocca GT, Saratti CM, Poncet A, Feilzer AJ, Krejci I. The influence of FRCs reinforcement on marginal adaptation of CAD/CAM composite resin endocrowns after simulated fatigue loading. Odontology. 2016;104(2):220-32. https://doi.org/10.1007/s10266-015-0202-9. PMid:25854165.
6. Weir MD, Ruan J, Zhang N, Chow LC, Zhang K, Chang X, et al. Effect of calcium phosphate nanocomposite on in vitro remineralization of human dentin lesions. Dent Mater. 2017;33(9):1033-44. https://doi.org/10.1016/j.dental.2017.06.015. PMid:28734567.
7. Heintze SD, Ilie N, Hickel R, Reis A, Loguercio A, Rousson V. Laboratory mechanical parameters of composite resins and their relation to fractures and wear in clinical trials: A systematic review. Dent Mater. 2017;33(3):e101-14. https://doi.org/10.1016/j.dental.2016.11.013. PMid:27993372.
8. Dybvik T, Leknes KN, Bøe OE, Skavland RJ, Albandar JM. Bioactive ceramic filler in the treatment of severe osseous defects: 12-month results. J Periodontol. 2007;78(3):403-10. https://doi.org/10.1902/jop.2007.060263. PMid:17335363.
9. Shah S, Shilpa-Jain D, Velmurugan N, Sooriaprakas C, Krithikadatta J. Performance of fibre reinforced composite as a post-endodontic restoration on different endodontic cavity designs: an in-vitro study. J Mech Behav Biomed Mater. 2020;104:103650. https://doi.org/10.1016/j.jmbbm.2020.103650. PMid:32174408.
10. Elmatary A, Moawad E, Heidarifar O, Stone S. Endodontic access cavity preparation: challenges and recent advancements. Br Dent J. 2025;238(7):469-75. https://doi.org/10.1038/s41415-025-8442-8. PMid:40217029.
11. Kurmaena IE, Nurliza C, Gani BA. Effect of 17% ethylenediaminetetraacetic acid and silver citrate on sealer resin penetration in the apical third. Dent J. 2024;57(3):178-83. https://doi.org/10.20473/j.djmkg.v57.i3.p178-183.
12. Abidin T, Susilo D, Gani BA. The effectiveness of nano-chitosan high molecular 0.2% as irrigant agent against Enterococcus faecalis with passive ultrasonic irrigant. J Conserv Dent. 2022;25(1):37-41. https://doi.org/10.4103/jcd.jcd_437_21. PMid:35722074.
13. Soraya C, Syafriza D, Andriany P, Jakfar S, Gani BA. Cellular response of chitosan loligo sp to changes in cell metabolism of Enterococcus faecalis. Trop J Nat Prod Res. 2025;9(3):1324.
14. Gani BA, Asmah N, Soraya C, Syafriza D, Rezeki S, Nazar M, et al. Characteristics and antibacterial properties of film membrane of chitosan-resveratrol for wound dressing. Emerg Sci J. 2023;7(3):821-42. https://doi.org/10.28991/ESJ-2023-07-03-012.
15. Mu P, Li X, Yang L, Cui C, Zheng W, Wang J, et al. The effect of joint filling materials on crack propagation under dynamic load. Mech Adv Mater Structures. 2025;1-14. https://doi.org/10.1080/15376494.2025.2467236.
16. Garoushi S, Säilynoja E, Frater M, Keulemans F, Vallittu PK, Lassila L. A comparative evaluation of commercially available short fiber-reinforced composites. BMC Oral Health. 2024;24(1):1573. https://doi.org/10.1186/s12903-024-05267-6. PMid:39736654.
17. Selvaraj H, Krithikadatta J, Shrivastava D, Onazi MAA, Algarni HA, Munaga S, et al. Systematic review fracture resistance of endodontically treated posterior teeth restored with fiber reinforced composites- a systematic review. BMC Oral Health. 2023;23(1):566. https://doi.org/10.1186/s12903-023-03217-2. PMid:37574536.
18. Valizadeh S, Ranjbar Omrani L, Deliperi S, Sadeghi Mahounak F. Restoration of a nonvital tooth with fiber reinforce composite (wallpapering technique). Case Rep Dent. 2020;2020(1):9619787. https://doi.org/10.1155/2020/9619787. PMid:32566326.
19. Monazami M. Multiphase characteristics of carbon fiber-reinforced cementitious materials under static and freeze-thaw cyclic loading conditions [dissertation]. Victoria: University of Victoria; 2023.
20. Guo G, Fan Y, Zhang JF, Hagan JL, Xu X. Novel dental composites reinforced with zirconia-silica ceramic nanofibers. Dent Mater.

2012;28(4):360-8. https://doi.org/10.1016/j.dental.2011.11.006. PMid:22153326.

21. Thaker S, Botchu R, Gupta H. Insights into obtaining FRCR and beyond: obstacles, opportunities and post-relocation dilemma–An Indian perspective. Indian J Radiol Imaging. 2020;30(1):70-6. https://doi.org/10.4103/ijri.IJRI_438_19. PMid:32476753.

22. Li X, Guo Z, Huang Q, Yuan C. Research and application of biomimetic modified ceramics and ceramic composites: a review. J Am Ceram Soc. 2024;107(2):663-97. https://doi.org/10.1111/jace.19490.

23. Jiang L, Zhou Y, Jin F. Design of short fiber-reinforced thermoplastic composites: a review. Polym Compos. 2022;43(8):4835-47. https://doi.org/10.1002/pc.26817.

24. Al Hatem O. Evaluating surface roughness and microbial adhesion to four provisional prosthodontic restorative materials. Houston: The University of Texas School of Dentistry; 2022.

25. Geng Z, Huang N, Castelli M, Fang F. Polishing approaches at atomic and close-to-atomic scale. Micromachines (Basel). 2023;14(2):343. https://doi.org/10.3390/mi14020343. PMid:36838045.

26. Restrepo A, Andrés C, Torres-López A, Correa F, Ardila C. Effect of two multi-step polishing systems on surface characteristics of nanohybrid composite resins: influence of reuse. J Clin Exp Dent. 2025;17(8): e929-35. https://doi.org/10.4317/jced.62873. PMid:40950512.

27. Mohamed MH, Abouauf EA, Mosallam RS. Clinical performance of class II MOD fiber reinforced resin composite restorations: an 18-month randomized controlled clinical trial. BMC Oral Health. 2025;25(1):159. https://doi.org/10.1186/s12903-025-05521-5. PMid:39881262.

28. Ibrahim RH, ElKassas DW, Nabih SM, Salem MN, Haridy R. The impact of different fiber placement techniques on the fracture resistance of premolars restored with direct resin composite, in vitro study. J Funct Biomater. 2025;16(6):225. https://doi.org/10.3390/jfb16060225. PMid:40558911.

29. Hahn B, Haubitz I, Krug R, Krastl G, Soliman S. Influence of matrix type on marginal gap formation of deep class II Bulk-Fill Composite Restorations. Int J Environ Res Public Health. 2022;19(9):4961. https://doi.org/10.3390/ijerph19094961. PMid:35564356.

30. Satterthwaite JD, Maisuria A, Vogel K, Watts DC. Effect of resin-composite filler particle size and shape on shrinkage-stress. Dent Mater. 2012;28(6):609-14. https://doi.org/10.1016/j.dental.2012.01.007. PMid:22342645.

31. Vahidi B, Alaghehmand H, Tashakkorian H, Seyedmajidi S, Ghasempour M. Effect of glass ionomer filler size on fluoride release, antiplaque properties, and abrasive effects of toothpaste. Clin Exp Dent Res. 2025;11(1):e70109. https://doi.org/10.1002/cre2.70109. PMid:40066482.

32. AlJarboua RT, Alshihry RA, Alkhaldi HO, Al Marar FH, Aljaffary MA, Almana ML, et al. Effect of fiber-reinforced composite placement site on fracture resistance of premolar teeth: an in vitro study. Clin Cosmet Investig Dent. 2024;16:255-66. https://doi.org/10.2147/CCIDE.S461134. PMid:39006828.

33. Alghalayini S, Ebeid KK, Aldahrab A, Wahsh M. Fracture load of nano-ceramic composite material for anterior endocrown restorations. Braz Dent Sci. 2020;23(1):9. https://doi.org/10.14295/bds.2020.v23i1.1853.

34. El Shazli MM, El-Etreby A, Mohamed FA. Effect of repeated pressing on the fracture resistance of heat-pressed glass ceramic crowns. Braz Dent Sci. 2024;27(3):e4267. https://doi.org/10.4322/bds.2024.e4267.

35. Reis DP, Noronha JD Fo, Rossi AL, de Almeida Neves A, Portela MB, da Silva EM. Remineralizing potential of dental composites containing silanized silica-hydroxyapatite (Si-HAp) nanoporous particles charged with sodium fluoride (NaF). J Dent. 2019;90:103211. https://doi.org/10.1016/j.jdent.2019.103211. PMid:31622646.

36. Sadasivuni KK, Saha P, Adhikari J, Deshmukh K, Ahamed MB, Cabibihan J-J. Recent advances in mechanical properties of biopolymer composites: a review. Polym Compos. 2020;41(1):32-59. https://doi.org/10.1002/pc.25356.

37. Goteti SV, Anwarullah A, Mandava J, Kantheti S, Pulidindi H, Chandolu V. Evaluation of microtensile bond strength and marginal adaptation of fiber-reinforced composites. J Conserv Dent Endod. 2024;27(11):1120-5. https://doi.org/10.4103/JCDE.JCDE_515_24. PMid:39777388.

38. Ren F, Ding Y, Leng Y. Infrared spectroscopic characterization of carbonated apatite: a combined experimental and computational study. J Biomed Mater Res A. 2014;102(2):496-505. https://doi.org/10.1002/jbm.a.34720. PMid:23533194.

39. El Ouarti I, Lotfi EM, Ben Ali M, Bouklouze A, Abdallaoui F. Enamel demineralization and remineralization pH cycling models in vitro: a SEM–EDX and FTIR study. Odontology. 2025;1-13. Ahead of print. https://doi.org/10.1007/s10266-025-01136-y. PMid:40579674.

40. Pires PM, Neves AA, Makeeva IM, Schwendicke F, Faus-Matoses V, Yoshihara K, et al. Contemporary restorative ion-releasing materials: current status, interfacial properties and operative approaches. Br Dent J. 2020;229(7):450-8. https://doi.org/10.1038/s41415-020-2169-3. PMid:33037365.

41. Alshetiwi DSD, Muttlib NAA, El-Damanhoury HM, Alawi R, Rahman NA, Elsahn NA, et al. Evaluation of mechanical properties of anatomically customized fiber posts using E-glass short fiber-reinforced composite to restore weakened endodontically treated premolars. BMC Oral Health. 2024;24(1):323. https://doi.org/10.1186/s12903-024-04102-2. PMid:38468269.

42. Almuhayya S, Alshahrani R, Alsania R, Albassam A, Alnemari H, Babaier R. Biofilm Formation on Three High-Performance Polymeric CAD/CAM Composites: An In Vitro Study. Polymers (Basel). 2025;17(5):676. https://doi.org/10.3390/polym17050676. PMid:40076168.

43. Li L, Khan M, Jiang X, Shakor P, Zhang Y. Editorial: sustainable fiber reinforced cementitious composites for construction and building materials. Frontiers. 2023:1237960. https://doi.org/10.3389/978-2-8325-3055-9.

44. Magne P, Carvalho MA, Milani T. Shrinkage-induced cuspal deformation and strength of three different short fiber-reinforced composite resins. J Esthet Restor Dent. 2023;35(1):56-63. https://doi.org/10.1111/jerd.12998. PMid:36629028.

45. Soares CJ, Faria-E-Silva AL, Rodrigues MP, Vilela ABF, Pfeifer CS, Tantbirojn D, et al. Polymerization shrinkage stress of composite resins and resin cements - What do we need to know? Braz Oral Res. 2017;31(suppl 1):e62. https://doi.org/10.1590/1807-3107bor-2017.vol31.0062. PMid:28902242.

46. Zhakiyeva Z, Magnin V, Poulain A, Campillo S, Asta MP, Besselink R, et al. How much water is there within calcium silicate hydrates? Probing water dynamics by Inelastic Neutron Scattering and Molecular Dynamics Simulations. ChemRxiv. 2023:1-38. Ahead of print. https://doi.org/10.26434/chemrxiv-2023-9zj33-v2.

Nurhayaty Natsir
(Corresponding address)
Hasanuddin University, Faculty of Dentistry,
Department of Dental Conservation, Makassar, South Sulawesi, Indonesia.
Email: nurhayatinatsir@unhas.ac.id

Editor-in-chief: Sergio Eduardo de Paiva Gonçalves
Editor: Amanda Maria de Oliveira Dal Piva

Date submitted: 2025 Sept 20
Accept submission: 2026 Feb 10